Contents list available at IJRED website

Int. Journal of Renewable Energy Development (IJRED)

Journal homepage: https://ijred.undip.ac.id

Research Article

Synthesis and Characterization of Hydrochar and Bio-oil from Hydrothermal Carbonization of *Sargassum* sp. using Choline Chloride (ChCl) Catalyst

Heri Rustamaji[a,b], Tirto Prakoso[a*], Jenny Rizkiana[a], Hary Devianto[a], Pramujo Widiatmoko[a], Guoqing Guan[c]

[a] *Department of Chemical Engineering, Bandung Institute of Technology, Bandung, Indonesia*

[b] *Department of Chemical Engineering, Lampung University, Lampung, Indonesia*

[c] *North Japan Research Institute for Sustainable, Hirosaki University, Aomori, Japan*

Abstract. The purpose of this study is to alter the biomass of *Sargassum* sp. into elective fills and high valuable biomaterials in a hydrothermal process at 200°C for 90 minutes, using $ZnCl_2$ and $CaCl_2$ activating agents, with ChCl as a catalyst. This method generated three primary outputs: hydrochar, bio-oil, and gas products. ChCl to water ratio varies from 1:3, 1:1, and 3:1. The hydrochar yield improved when the catalyst ratio was increased, but the bio-oil and gas yield declined. The highest hydrochar yields were 76.95, 63.25, and 44.16 percent in $ZnCl_2$, $CaCl_2$, and no activating agent samples, respectively. The porosity analysis observed mesopore structures with the most pore diameters between 3.9-5.2 nm with a surface area between 44.71-55.2. The attribute of interaction between activator and catalyst plays a role in pore formation. The hydrochar products with $CaCl_2$ showed the best thermal stability. From the whole experiment, the optimum hydrochar yield (76.95%), optimum surface area (55.42 $m^2\ g^{-1}$), and the increase in carbon content from 21.11 to 37.8% were achieved at the ratio of ChCl to water was three, and the activating agent of $ZnCl_2$. The predominant bio-oil components were hexadecane, hexadecanoic, and 9-octadecenoic acids, with a composition of 51.65, 21.44, and 9.87%, respectively the remaining contained aromatic alkanes and other fatty acids. The findings of this study reported that adding activating agents and catalysts improve hydrochar yield and characteristics of hydrochar and bio-oil products, suggesting the potential of hydrochar as a solid fuel or biomaterial and bio-oil as liquid biofuel.

Keywords: *Sargassum* sp.; Hydrothermal carbonization; Carboneous material; Activating agent; Platform chemical

Article history: Received: 12th Nov 2021; Revised: 28th Dec 2021; Accepted: 6th January 2022; Available online: 20th January 2022
How to cite this article: Rustamaji, H., Prakoso, T., Rizkiana, J., Devianto, H., Widiatmoko, P., and Guan, G. (2022). Synthesis and Characterization of Hydrochar and Bio-oil from Hydrothermal Carbonization of *Sargassum* sp. using Cholin Chloride (ChCl) Catalyst. *International Journal of Renewable Energy Development,* 11(2), 403-412.
https://doi.org/10.14710/ijred.2022.42595

1. Introduction

Seaweed is among the most predominant organic resources in Indonesian waters, and its variety shows a stark significant contrast compared to other nations. This biomass demonstrates the most significant contribution to the overall production of the country's aquaculture and is also perceived as an increasing economic driver (Purnomo *et al.* 2020, Kambey *et al.* 2020). However, marine growth utilization appears highly restricted, with a large portion serving as food sources, such as agar and carrageenan, without any conversion. Approximately 80% of Indonesia's seaweed exports to China, South Korea, and Vietnam comprise low valuable dried raw materials (Saleh & Sebastian 2020).

There is a need to streamline the excellent accessibility of seaweed in Indonesian oceans by transforming the species into other valuable forms, including biochemical, biomaterial, and biofuel products. Using hydrothermal carbonization (HTC), this conversion process attracts wider attention and consideration. The hydrothermal reaction in water occurs at a high temperature and pressure range of 180-347°C and 4-22 MPa, respectively. Also, its main objectives include utilizing raw materials with high dampness and pre-drying requirement (Tekin *et al.* 2014, Prakoso *et al.* 2018). Consequently, the hydrothermal technique appears appropriate for seaweed preparation due to its excellent dampness value.

The hydrothermal method generated three primary products: hydrochars (HC), bio-oil, and biogas. This process typically uses activating agents such as KOH, H_3PO_4, $ZnCl_2$, and $CaCl_2$ (Jain *et al.,* 2015). Catalysts, including choline chloride (ChCl), are also added to obtain precious liquid products (Bayu *et al.,* 2018). Xu *et al.* (2013) used HTC to produce hydrochar from Sargassum horneri utilized citric acid monohydrate as a catalyst. They found

* Corresponding author: tirto@che.itb.ac.id

that reaction temperature, reaction time, and particle size were the essential parameters that affected hydrochar properties. Smith and Ross (2016) investigate the seasonal variations in seaweed to the composition effect of solid fuel quality by the HTC process and show that the highest energy yields are obtained in the summer and autumn harvested algae.

Zheng *et al.* (2018) found that the HTC of S. horneri at 180°C for two hours is suitable for HC production with a high yield and macroporous structure. Brown *et al.* (2020) investigated the integration of HTC and anaerobic digestion (AD) as a valorization route for two seaweed species. They explained that treatment at 150 °C, with separate product utilization, can increase the energetic output of S. latissima and F. serratus by 47 percent and 172 percent, respectively, when compared to digestion of untreated macroalgae. Patel *et al.* (2021) examined the effects of the HTC process conditions on the yield and the properties of the hydrochar and process water from seaweed. The hydrochar produced at 220°C and 120 min showed the highest carbon content (48.5%) and heating value (18.93 MJ/kg).

Previous HTC seaweed research has not addressed the effect of using other activation agents such as $ZnCl_2$ and $CaCl_2$, ChCl catalysts, and the composition of liquid products. This study examines the properties of hydrochar and liquid products from the hydrothermal process of seaweed using $ZnCl_2$ and $CaCl_2$ activating agents with a ChCl catalyst. $ZnCl_2$ and $CaCl_2$ can act as dehydrating agents that will improve the characteristics of hydrochar products. At the same time, ChCl is an ionic solution catalyst expected to enhance hydrochar yield and direct reactions pathways to produce high-value platform chemicals.

2. Materials and Methods

2.1 Materials

This study employed seaweed (*Sargassum* sp.) from Jepara, Central Java, as the raw material. The $ZnCl_2$ and $CaCl_2$ activating agents were purchased from Merck, ENSURE (>99%), the choline chloride (ChCl) catalyst was purchased from Salus Nutra Inc., Xian, China, while fiber filter paper was obtained from GF/B, Whatman.

2.2 Methods

2.2.1 Hydrothermal Carbonization

The biomass samples were dried at 105°C for 24 hours, then grinded and sieved to get a 0.4 mm particle size. The hydrothermal carbonization of *Sargassum* sp was conducted in an autoclave batch reactor of 200 mL volumetric capacity. About 2.4 g of the species and 1.4 g of $CaCl_2$ and $ZnCl_2$ were constant. Meanwhile, the ChCl catalyst was combined with demineralized water to obtain ratios 1:3, 1:1, and 3:1 by weight solutions with the total mixture at 128 g. The biomass and activating agents were then introduced into the ChCl solution and placed in the hydrothermal reactor to be processed for 90 minutes at 200°C (Titirici 2013). After cooling through the sampling valve, the gaseous product removal followed the sampling bag. Also, the resulting mixture was collected and filtered to separate the solid and liquid portions, termed hydrochar and liquid fraction, respectively. The hydrochar (HC) was then dried overnight at 105°C, while the water content in the liquid fraction was separated by vacuum distillation, the residue termed bio-oil.

2.2.2 Characterization of Product

Several methods were used to characterize the solid product. The *Sargassum* sp. and hydochar composition were assessed in the Coal Testing Laboratory of tekMIRA Bandung, using ultimate (ASTM: D5868-10a) and proximate (ASTM: D-3175) analysis. BET surface area and pore volume obtained by a gas sorption system Nova 3200e from Quantochrome machines in the Instrumentation Laboratory of Chemical Engineering, Bandung Institute of Technology. The specific surface area was calculated using the Brunauer–Emmet–Teller (BET) method. The total pore volume was calculated using the adsorption amount at a relative pressure of 0.9. In contrast, the pore size distributions (PSD) were calculated using the Barrett–Joyner–Halenda (BJH) method. Hydrochar morphology was subsequently investigated in the Center for Research in Nanoscience and Nanotechnology Bandung Institute of Technology, using scanning electron microscopy (SEM) with a Hitachi SU3500 SEM (Prakoso *et al.,* 2018).

The TGA apparatus was used to conduct thermogravimetric analysis of *Sargassum* sp. and hydrochar samples (100 mg) (Q50, TA Instrument, New Castle, USA). Nitrogen served as the carrier gas at a flow rate of 25 ml min^{-1}. Operating temperature between 30-1000°C and heating rates were monitored at five incremental from 5-20°C min^{-1}. The infrared vibrational mode of the samples was obtained at an average of 24 sweeps by a Nicolet 6700 FTIR spectrometer ranging 5000-400 cm^{-1} with unearthly reach at 4 cm^{-1} goals, and a KBr pellet was used as a perspective example. Furthermore, a PANalytical XPert PRO diffractometer with Cu-K radiation collected the XRD designs (40 kV, 40 mA).

Bio-oil from the HTC process with the activating agent $ZnCl_2$ and the ratio of ChCl to water three were used as the GC-MS analysis sample. Concentrated bio-oil was dissolution in a ratio of 1 to 100, using acetone. Subsequently, the diluted bio-oil was injected into a GC-MS machine (GCMS-TQ8050 NX) using a Shimadzu RTX 5 ms capillary column to determine its composition. Helium was used as the carrier gas at a flow rate of 1 ml min^{-1}. The experiment was carried out at a column temperature of 40-295°C, with a heating rate of 5°C min^{-1} and 20 minutes holding period.

The yield of wet solid, liquid, gas and hydrochar were calculated using equations (1)-(4) (Patel *et al.,* 2021).

$$Solid\ Yield\ (\%) = \frac{Mass\ of\ wet\ solid}{Mass\ of\ feedctock} \cdot 100\% \quad (1)$$

$$Liquid\ Yield\ (\%) = \frac{Mass\ of\ liquid}{Mass\ of\ feedctock} \cdot 100\% \quad (2)$$

$$Gas\ Yield\ (\%) = 100 - Solid\ Yield - Liquid\ Yield \quad (3)$$

$$Hydrochar\ Yield\ (\%) = \frac{Mass\ of\ dried\ hydrochar}{Mass\ of\ dried\ raw\ seaweed} \cdot 100\% \quad (4)$$

3. Results and Discussion

3.1. Sargassum sp. *and Hydrochar Characterization*

The elemental composition of seaweed and hydrochar samples was obtained in the ultimate analysis. Table 1 represents the ultimate and proximate analyses of *Sargassum* sp. and hydrochar. The seaweed showed significant levels of oxygen and carbon, while the quantity of the volatile matter was higher than the fixed carbon, moisture, or ash. However, due to the increased alkali content, the seaweed exhibited an extensive ash content than other biomasses (Smith & Ross 2016). Consequently, thermochemical procedures such as direct combustion, pyrolysis, and gasification proved inefficient (Tirto *et al*., 2018). These characteristics appeared more acceptable during the hydrothermal method. Compared to crude samples, hydrochars are recognized for lowering moisture and ash composition and increasing volatile materials and fixed carbon due to the proximate analysis. In addition, carbon remains inadequately degraded but may serve as a storage or reservoir for carbon emissions. The hydrochar moisture content decreased from 14.4 to 5.5% in the raw material, indicating that the HTC process produced a more hydrophobic surface (Xu *et al.,* 2013).

The raw material contained 14.6% ash, which was reduced to 8.5% in the resulting hydrochars. Soluble inorganic fractions such as alkali metals and earth salts were quickly removed, leading to lower ash content. Also, the carbon composition increased from 21.11 to 37.8% in the hydrochar samples, indicating hydrochar carbon concentration is highly reliant on hydrothermal processing conditions (200°C, activating agent of $ZnCl_2$, and ChCl to water is three) and the carbon content of seaweed.

3.2. Product Yield

Table 2 shows the product yield using various activating agents and ratio variations between choline chloride and water. This representation provides sufficient information on the activating agents' effect on hydrochar and bio-oil results—the most significant hydrochar product at a ChCl to water at three uses $ZnCl_2$. Khan *et al*. (2019) reported that the biomass HTC process has a complicated reaction network in which hemicellulose, cellulose, and lignin are subjected to a series of reactions. The reaction begins with hydrolysis, dehydration, and decarboxylation to produce water-soluble intermediates. Dehydration was the immediate reaction in the activating agent presence in cellulose or lignocellulose precursors. Hydrochar is produced by polymerizing the reactive intermediates and solid-solid converting solid residues (Titirici, 2013; Jain *et al*., 2015). In addition, during heat treatment, the activating agent of $ZnCl_2$ and $CaCl_2$ were responsible for biomass dehydration, removing hydrogen and oxygen as water rather than CO_x or hydrocarbons, preventing the loss of volatile materials and tars and leaving more fixed carbon behind, enhanced solid formation and, consequently, a higher reaction hydrochar yield (Wang *et al*., 2018).

Although $ZnCl_2$ and $CaCl_2$ are dehydrated agents in biomass, $CaCl_2$ has a more robust adsorption capacity. It acts as an expansive agent, infiltrating the biomass framework to create large pores, but its dehydrating effects and ability to limit tar formation are less than $ZnCl_2$ (Peng *et al*., 2016). This phenomenon explains that $CaCl_2$, in general, has a lower hydrochar yield than $ZnCl_2$ (Li *et al*., 2021).

Furthermore, the higher ratio of ChCl: water increases the hydrochar yield but decreases the liquid recovery. ChCl is a non-reactive, water-free, non-volatile, biodegradable ionic liquid known as deep eutectic solvents (DESs). According to Carriazo *et al*., (2012), ChCl served as a fluid medium for reactant homogenization, a structure-directing agent for a hierarchically porous structure, and a carbon supply in the synthesis process. The ChCl also serves as the medium for precursor, template, or reactor to manufacture the desired material with a unique morphology or chemical constituent. This role is believed to improve the solid yield of the hydrothermal carbonization reaction (Carriazo *et al*., 2012). Consequently, the hydrochar yield in the present study appeared higher, compared to the previous investigation, such as 46.9, 52.3, and 39% by Patel *et al.* (2021), Xu *et al.* (2013), and Smith & Ross (2016), respectively.

3.3. Hydrochar Porosity

Figure 1. shows the nitrogen adsorption/desorption isotherm curves for each hydrochar with ChCl to water ratio is 3. Porosity is generally classified based on pore size and access (open versus closed). The International Union of Pure and Applied Chemistry (IUPAC) recommendations state that porous materials are categorized by dry pore size. Micropores, mesopores, and macropores exhibit pores below 2, between 2-50 and above 50 nm, respectively. Nanoporous substances are frequently used to describe porous thin films or materials produced using a block copolymer method. However, nanopores exclusively refer to pores with a diameter below 100 nm (Titirici, 2013).

Table 1
Ultimate and proximate analysis of S*argassum* sp. and hydrochar.

	Ultimate (wt%)					Proximate (wt%)			
Sample	C	H	N	O	S	FC	VM	MC	Ash
S*argassum* sp.	21.11	4.26	0.35	56.73	2.9	9.6	61.4	14.4	14.6
Hydrochar†	37.80	5.10	1.40	46.20	1.40	23.0	63.0	5.50	8.50

C: carbon, H: hydrogen, N: nitrogen, O: Oxygen, S: Sulfur, FC: Fixed carbon, VM: volatile matter, MC: moisture content.
†Activating agent of $ZnCl_2$, ChCl to water ratio is 3.

Table 2
Product yield from the hydrothermal carbonization process

Process Variable		Product Yields			
Activating Agent	ChCl water	Solid yield (%)	Liquid yield (%)	Gas yield (%)	Hydrochar yield (%)
None	1:3	3.7	88.4	7.9	19.67
$CaCl_2$	1:3	4.2	88.3	7.5	22.67
$ZnCl_2$	1:3	4.5	88.1	7.4	24.53
None	1:1	6.3	87.3	6.4	33.80
$CaCl_2$	1:1	6.5	87.2	6.3	35.32
$ZnCl_2$	1:1	6.9	87.4	5.7	37.43
None	3:1	8.2	86.8	5.0	44.16
$CaCl_2$	3:1	11.7	83.5	4.8	63.25
$ZnCl_2$	3:1	14.2	80.9	4.9	76.95

The pore volume, pore size distribution, and porosity are all critical parameters to consider, in addition to BET surface area. Figure 1 shows one wide hysteresis loop at (0.1 < P/Po < 0.93). Based on IUPAC, the curve of the three samples belongs to type IV, which is associated with capillary condensation, which characterizes the hierarchy of mesoporous structures with highly content. High N_2 adsorption capacities imply high surface areas and large pore volumes (Zhang *et al.,* 2020). In this case the absorption capacity of N_2 is sequentially ZnI_2 > $CaCl_2$ > no activation agent. The mesoporous structure of hydrochar is further confirmed by the pore size distribution plot in Figure 2, which shows the pore diameter of hydrochar in the wide range of 3.6 - 40 nm. The three samples in Figure 2 had a pore sizes distribution with different narrow peaks at about 3.6-5 nm, which verified the effect of adding activation agents to the pore structure (Yu *et al*., 2021).

Table 3 shows the average pore diameter, surface area, and total pore volume of the hydrochar sample. The specific surface area and pore volume of the hydrochar gradually increase with an activating agent. The BET surface area of hydrochar without activating agent (44.14 m^2g^{-1}) is slightly lower than those of hydrochar with an activating agent of $CaCl_2$ (52.63 m^2g^{-1}) and $ZnCl_2$ (55.42 m^2g^{-1}). Likewise, the pore volume increased for hydrochar without activating agent, $CaCl_2$, and $ZnCl_2$, each with a value of 0.12; 0.13, and 0.14 cm^3g^{-1}. Meanwhile, hydrochar with $CaCl_2$ activation agent showed the highest average pore diameter with a value of 5.26 nm. $ZnCl_2$ and $CaCl_2$ create porosity because of the spaces left by the activating agent after the washing stage (template behavior). Due to the small size of the $ZnCl_2$ molecule or its hydrates, the mesopores formed are small and homogeneous in size. $CaCl_2$, on the other hand, has a greater adsorption capacity. It acts as an expander, permeating the biomass structure and generating larger pores (Jeong *et al.,* 2011).

The seaweed hydrochar showed a larger BET surface area of 21 $m^2\ g^{-1}$, compared to other biomasses, such as pinewood (1.4 $m^2\ g^{-1}$), *enteromorpha prolifera* (1.4 $m^2\ g^{-1}$) and maize silage (12 $m^2\ g^{-1}$) (Liu *et al.* 2010). This is due to the particular framework of *Sargassum* sp. and the introduction of activating agents.

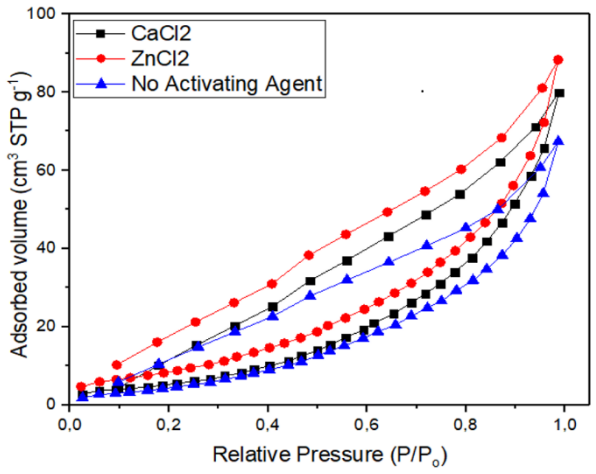

Fig 1. Nitrogen adsorption–desorption isotherms for ChCl to water ratio is 3

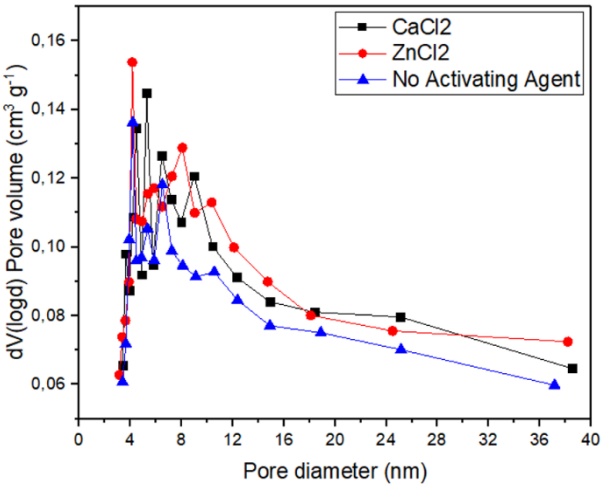

Fig 2. Pore size distribution of hydrochar products for ChCl to water ratio is 3

Table 3
Pore size diameter, surface area, and total pore volume of hydrochars for ChCl to water ratio is 3

Hydrochar Sample	Pore Diameter (nm)	BET Surface Area (m^2g^{-1})	Total Pore Volume (cm^3g^{-1})
No activating agent	4.14	44.78	0.12
Activating agent, $CaCl_2$	5.26	52.63	0.13
Activating agent, $ZnCl_2$	3.90	55.42	0.14

3.4. Thermogravimetric Analysis

Figure 3 illustrates the thermogravimetric (TG) and differential thermogravimetric (DTG) analysis seaweed and hydrochar curves synthesized from *Sargassum sp.* at 200°C and 1:1 solvent ratio. The thermal decomposition characteristics of hydrochar were significantly unique compared to the seaweed feedstock. In the case of seaweed (Figure 3. a), the initial stage of thermal degradation occurred between 35-250°C, with a single pinnacle focused at 70°C, because of the evaporation of the surface water (Smith & Ross 2016, Xu *et al.* 2013).

In the subsequent phase, a massive decrease in material load of approximately 38% was observed within 200-400°C, relating to the disintegration of the biopolymer portion (Kim *et al.,* 2013). Furthermore, two broad pinnacles were identified between 200-350°C. The leading (200-280°C) and the second (below 350°) tops were possibly related to the crumbling of starches and proteins, while the warm debasement design resembled the macro-algae described by Li *et al.* (2016). However, the weight decline in the last stage from 400-800° tends to be identified with lignin and the remaining protein (Wei *et al.,* 2018).

In terms of hydrochar, the significant mass decrease occurred between 200-400°C. Figure 3b shows only one sharp peak at 350°C, indicating that the biopolymer fraction, mainly hemicellulose, had broken down after the HTC process. A comparable phenomenon was observed in different examinations (Gao *et al.* 2018), where a mixture of hydrochar and $CaCl_2$ demonstrated the sharpest peaks. This shows that the hydrochar from $CaCl_2$ activation obtained the best thermal stability. However, a significant reduction in mass was recorded at the last stage above 600°C, indicating that the activating agent carved the carbon to form an overall porous structure (Luo *et al.,* 2018). Consequently, the thermal characteristics of hydrochar synthesized with or without an activating agent appeared relatively similar.

3.5. Morphological and Structural Characterization

Scanning electron microscopy (SEM) characterized the morphologies of *Sargassum* sp. and hydrochar from the process with the catalyst to water ratio three was characterized by scanning electron microscopy (SEM). Figure 3 represents the SEM images used to examine the morphological changes on the surface and physical properties of the raw *Sargassum* sp. and hydrochar. Based on the illustration, raw *Sargassum* sp. showed a typical cellular structure of lignocellulosic biomass with irregular shapes resembling block and closed surface. However, the lignocellulosic frame was cracked into a piece due to the HTC interaction. Particular tiny pores created by gas emanation were attributed to the unpredictable matter in the hydrochar (Fig. 4.b). During the hydrothermal process at a temperature of 200oC, microparticles such as minimally separated circles remain together outside the lignocellulosic.

The hydrochar obtained specific morphological shapes after the hydrothermal process. Figures 4. b-d show the hydrochar microscopic particles and the elongated structures in the agglomerates. These structures were most certainly generated due to the sequential treatment. Non-uniform arrangements were also observed in the agglomerated particles. The mesopores tend to evolve from natural vascular channels used to transport water based on particular theories. Only a few nanoscales pore on the hydrochar surface, indicating low porosity (Luo *et al.* 2018).

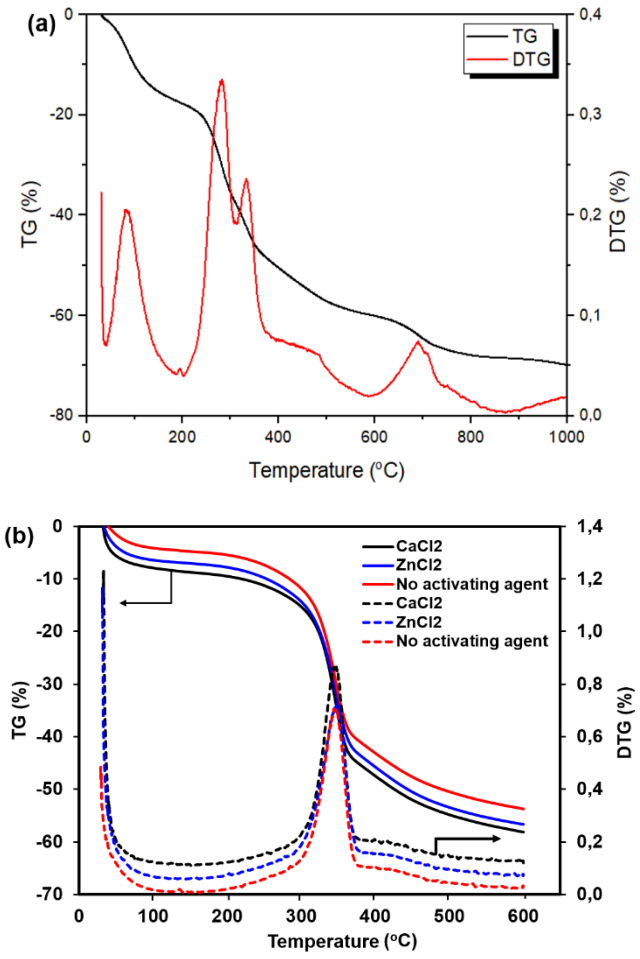

Fig 3. TG and DTG analysis of (a) seaweed and (b) hydrochar products for ChCl to water ratio is 3.

Furthermore, two methods were applied to classify the mechanism and reaction pathway of hydrochar production. The reaction includes the immediate, intensive transformation of non-dissolved lignin and cellulose, represented as a distinct response in the SEM data (Demir *et al.,* 2015). Figure 4. b shows hydrochar has a rougher surface which shows that the pore structure in hydrochar is formed with interconnected pore clusters. The sample has an irregular granular morphology with large pores on the surface (Zhu et al., 2018). Figure 4. c shows the morphology of hydrochar with a loose and interconnected structure with interstitial porosity and uniformly distributed and many small sizes indicating a larger surface area. Figure 4.d shows that the hydrochar sample displays a related porous network structure with uneven wrinkles, which means a smaller surface area as the results of the porosity analysis (Dai et al., 2018)

The hydrochar structures were studied comprehensively using X-ray diffraction (XRD). Figure 5 shows the samples of hydrochar from the process with the catalyst to water ratio three. The sharp diffraction peak at $2\theta = 20.38^{o}$ indicates the loss of the cellulose peak due to the hydrothermal process at 200°C. Sharp diffraction peak at $2\theta = 22.74^{o}$ corresponding to turbostratic order phases and amorphous ones indicates that *Sargassum* sp. was successfully carbonized to a carbon form (Khan et al., 2019). While the sharp peaks at $2\theta = 25.98^{o}$, 27.09^{o}, 28.3^{o}, 32.76^{o}, 34.32^{o}, 40.9^{o}, 42.98^{o}, 47.09^{o}, and 56.00^{o} in Figure 5 reflect inorganic components derived from seaweed ash content (Clemente *et al*., 2018). The peaks are per the results of the X-Ray Fluorescence (XRF) analysis of raw seaweed and hydrochar (Figure S1), which shows the content of several minerals such as Ca, Mg, Al, Fe, Si, K, Na, and Cl. This mineral is not entirely dissolved during the hydrothermal carbonization process and is not completely lost during the washing of the hydrochar with water. Hydrochar without activating agent had the highest crystallinity fraction and then decreased with CaCl and $ZnCl_2$ activating agents. At $2\theta = 20.38^{o}$ and $2\theta = 22.74^{o}$ diffraction, the hydrochar sample without an activating agent had the highest intensity, indicating that adding an activating agent tends to increase the destructive ability of seaweed cellulose crystallinity and decrease the percentage of hydrochar crystallinity (Nizamuddin et al., 2019). The three samples' crystalline and amorphous carbon fractions were 63:37, 49:51, and 47.3:52.7%, respectively, as shown in Figure S2-S4.

Hydrochar with $ZnCl_2$ activation agent showed the lowest crystallinity fraction because $ZnCl_2$ had the most significant defect effect, contributing to amorphous structures and the most considerable porosity. This result is consistent with the highest surface area of the three samples (Titirici, 2013). Satlewal *et al.* (2018) stated that the overall biomass crystallinity increased significantly at low temperature after DESs processing due to amorphous hemicellulose and lignin elimination. Similar events were believed to also occur in the hydrochar products processed with DES.

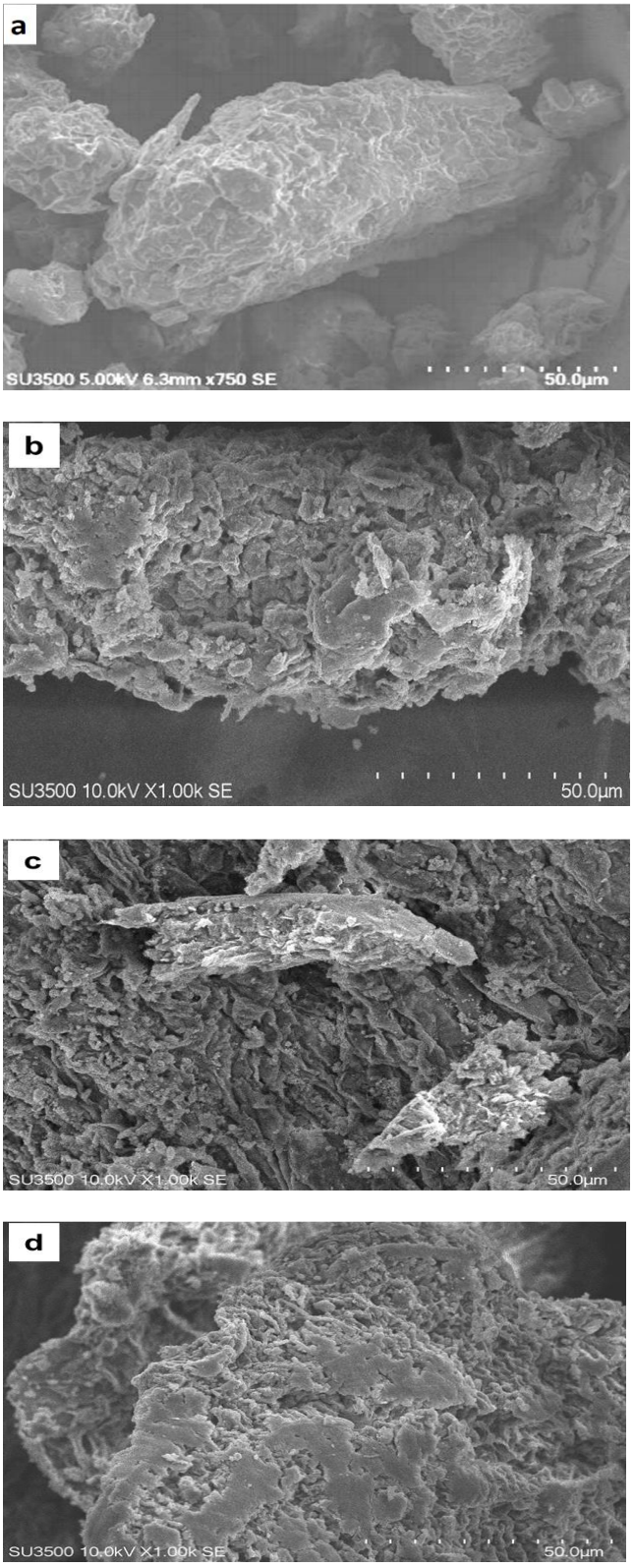

Fig 4. SEM Image of (a) *Sargassum* sp. and hydrochar with the activating agent of (b) $CaCl_2$, (c) $ZnCl_{2,\ and}$ (d) no activating agent, for ChCl to water ratio is 3.

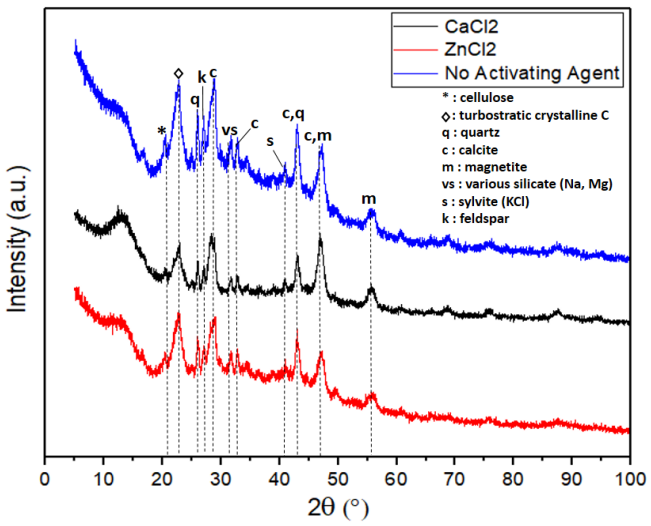

Fig 5. Analysis XRD pattern **of** hydrochar with an activating agent of $CaCl_2$, $ZnCl_2$, and no activating agent for ChCl to water ratio is 3.

Figure 6 represents the FTIR spectroscopy used to examine the functional groups of hydrochar. The adsorption peak between the 3000–3400 cm^{-1} sample region was linked to H-reinforced O-H vibration in the hydroxyl or carboxyl groups. Aliphatic C-H stretching was ascribed to the band at approximately 2920 cm^{-1}, indicating aliphatic compound formation during hydrothermal carbonization. Also, a C=O=C stretch was connected to the dip at around 2300 cm^{-1}, while the C=O peaked at 1650 cm^{-1} (Melo *et al*., 2016). The peak at 1650 cm^{-1}, suggesting the acidity is more attributed to the phenolic groups. However, the declining situation at 1400 cm^{-1} was due to C=C symmetrical bond, while C–OH was responsible for the dip at 1100 cm^{-1}. An out-of-plane C-Cl deformity vibration was associated with the bands between 500–800 cm^{-1} (Zhang *et al.,* 2012). Furthermore, the HC trademark pinnacles were consistent with the hydrochar from other biomass.

3.6. Bio-oil Composition

Table 4 displays the GCMS analysis results, with the majority of the bio-oil constituents being alkanes, aromatics, and fatty acids. Hexadecane obtained the optimal content of approximately 51.65% of the total area before hexadecanoic acid at 21.44%. The lignocellulosic biomass is initially hydrolyzed to glucose during hydrothermal carbonization, although specific proportions generate fructose.

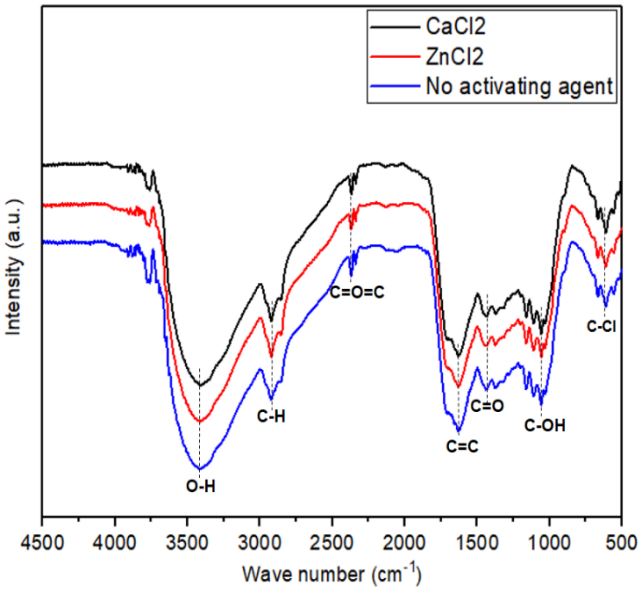

Fig 6. FTIR Spectra of hydrochar with an activating agent of $CaCl_2$, $ZnCl_2$, and no activating agent for ChCl to water ratio is 3.

Table 4
Compounds identified by GC–MS in. bio-oil produced by hydrothermal carbonization of *Sargassum* sp. for ChCl to water ratio is 3

No	RT‡ (min)	Area (%)	Component	Formula	Chemical Structure
1	5.356	1.89	Benzene-ethyl	C_8H_{10}	
2	20.871	4.26	nonanoic acid	$C_9H_{18}O_2$	
3	22.439	4.49	n-Pentadecane	$C_{15}H_{32}$	
4	24.844	51.65	Hexadecane	$C_{16}H_{34}$	
5	27.086	3.41	Heptadecane	$C_{17}H_{36}$	
6	29.218	3.00	Iron, tricarbonyl	$Fe(CO)_3$	
7	31.811	21.44	Hexadecanoic acid	$C_{96}H_{32}O_2$	
8	35.110	9.87	9-Octadecenoic acid (Z)-	$C_{18}H_{34}O_2$	

‡RT: Retention Time.

Organic acids such as levulinic acids are formed by decomposing glucose and fructose (Reza *et al.,* 2014). However, organic acids were not detected in this analysis. Consequently, aromatic compounds in the bio-oil, including ethylbenzene, must frame the aromatic compounds obtained from lignin to undergo intermolecular dehydration. Furthermore, the hydrolysis of triglycerides produces lipids in algae containing saturated and unsaturated fatty acids. Minimal alkanes are produced in the bio-oil due to the algae's fatty acids (Guo *et al.* 2015, Hadhoum *et al.* 2016).

Hexadecane is an alkane hydrocarbon with the chemical formula $C_{16}H_{34}$. Hexadecane (also called cetane) is a 16-carbon chain with three hydrogen atoms connected to each of the two ends and two hydrogen atoms bonded to each of the remaining 14 carbon atoms. The cetane number, a measure of the combustion of diesel fuel, is sometimes abbreviated as cetane. Because cetane ignites readily under compression, it is designated as cetane 100 and is used as a benchmark for other fuel combinations (Speight, 2015). Thus, the bio-oil product is a potential chemical platform for liquid biofuels.

3.7. Environmental Challenges and Energy Prospect

Hydrothermal treatment of lignocellulosic biomass is gaining popularity these days since it may transform the biomass into sustainable hydrochar and bio-oil in a short amount of time. Lignocellulose, glucose, agricultural residue, food waste, municipal solid waste, sewage sludge, aquaculture, and algal wastes were among the feedstocks chosen for HTC, ranging from model material to natural feedstock (Wang *et al.*, 2018). Hydrochar is a solid substance that is stable, hydrophobic, and friable, with a fuel value similar to lignite coal. Hydrochar offers many applications based on its properties, including solid fuel, syngas raw material, adsorbent, catalyst precursor, soil amendment, carbon sequestration, anaerobic digestion and composting additives, and material for electrochemical energy storage. Hydrochar has the potential to replace coal in existing coal-fired power plants. The processed solid is brittle and can be converted into pellets in a gasifier or coal power plant (Reza *et al.*, 2014).

Even though several studies on the use and activation of hydro charcoal and the improvement of bio-oil into fuel have been conducted, challenges and opportunities such as identifying and processing biomass with specific properties, the environmental impact of chemical activation, separation of bio-oil products based on compounds, and others still exist (Shen et al., 2021). The hydrochar surface composition, reactivity with the chemical activation agent, and yield are greatly affected by biomass with diverse chemical compositions (i.e., varying hemicellulose, cellulose, and lignin concentrations). HTC's hydrochar had a small surface area and porosity, which limited its applications in adsorption, electroconductivity, and the other regions. To improve the quality of hydrochar, it needed to expand existing pores and generate new pores using chemical activation (Zhang *et al.*, 2019). On the other side, after acid or alkaline treatment, a post washing of hydrochar is required for neutralization; the chemicals employed may pollute water or soil if not correctly treated, raising the cost. The activation method currently practiced using chemicals such as $ZnCl_2$ and $CaCl_2$ is an opportunity to replace the acid or base activator with a more effective and cheaper alternative (Jain *et al.*, 2015)

Techno-economic analysis (TEA) could help with future decision-making regarding the commercialization of lignocellulose hydrothermal treatment (Shen *et al.*, 2021). It also considers the costs of feedstock collection, equipment, operation, and manufacturing. Hydrochar is currently too expensive to compete with char made from fossil fuels (Kumar *et al.*, 2020). Hydrochar made from empty fruit bunches, for example, costs 7.9 € GJ^{-1}, which is significantly more than bituminous coal (2.6 € GJ^{-1}) (Stemann *et al.*, 2013). Despite this, HTC outperformed the other technologies in economic viability (HTC, pyrolysis, and anaerobic co-digestion) (Unrean *et al.*, 2018). Hydrochar is more cost-effective for co-firing than industrial wood pellets, which cost around 8.3 € GJ^{-1} in 2013 (Reza *et al.*, 2014). The present HTC TEA, on the other hand, is primarily based on data from lab-scale trials. Plants using large-scale continuous HTC reactors may have numerous distinctions from small and bench reactors, such as heat and mass transmission, separation methods, and so on (Akbari *et al.*, 2019, Shen *et al.*, 2021). Furthermore, the system with flash separators for steam heat recovery costs more (3.3 $ GJ^{-1}) than the plant with heat exchangers. As a result, it appears that the most cost-effective applications of HTC are for long-distance transport and long-term storage of biomass, as well as for wet biowastes. More research and analysis are needed to quantify the economic and longevity benefits of HTC hydrochar accurately.

4. Conclusion

This study showed that hydrochars (HC) and bio-oil are successfully produced from *Sagarssum* sp. by hydrothermal carbonization. The hydrochar yield improved when the catalyst ratio was increased, but the bio-oil and gas yield declined. The highest hydrochar yields in samples of $ZnCl_2$, $CaCl_2$, and without any activating agent were 77.91, 63.75, and 44.56%. The hydrochar material exhibited a mesoporous structure (3.9-5.2 nm) with a low surface area as the attribute of interaction between activator and catalyst play a role in pore formation. The best thermal stability of the hydrochar is obtained using $CaCl_2$ activation.

Furthermore, activating agents and catalysts promote the formation of graphitic structures in the hydrochars. The three most significant bio-oil components were hexadecane and hexadecanoic and 9-Octadecenoic acids covering 51.65, 21.44, and 9.87% of the entire region. The findings of this study reported that adding activating agents and catalysts improve hydrochar yield and characteristics of hydrochar and bio-oil products, suggesting the potential of hydrochar as a solid fuel or biomaterial and bio-oil as liquid biofuel.

Acknowledgment

The author is grateful to the Ministry of Research and Technology-National Research and Innovation Agency of

the Republic of Indonesia for funding this study under the research grant 2020.

References

Akbari, M., Oyedun, A.O., Kumar, A., 2019. Comparative energy and techno-economic analyses of two different configurations for hydrothermal carbonization of yard waste. *Bioresource Technology Reports*, 7, 1002103; doi.org/10.1016/j.biteb.2019.100210

Bayu, A., Yoshida, A., Karnjanakom, S., Kusakabe, K., Hao, X., Prakoso, T., Abudula, A., & Guan, G. (2018). Catalytic conversion of biomass derivatives to lactic acid with increased selectivity in an aqueous tin (II) chloride/choline chloride system. *Green Chemistry,* 40**,** 4112; doi.org/10.1039/C8GC01022F

Carriazo, D., Serrano, M. C., Gutiérrez, M. C., Ferrer, M .L., & del Monte, F. (2012). Deep-eutectic solvents play multiple roles in the synthesis of polymers and related materials. *Chemical Society Review*, 41, 4996-5014; doi.org/10.1039/C2CS15353J.

Clemente, J. S., Beauchemin, S., Thibault, Y., Ted MacKinnon, & Smith, D. (2018). Differentiating Inorganics in Biochars Produced at Commercial Scale Using Principal Component Analysis. *ACS Omega*, **3**, 6931−6944; doi.org/10.1021/acsomega.8b00523

Demir, M., Kahveci, Z., Aksoy, B., Palapati, N. K. R., Subramanian, A., Cullinan, H. T., Hani, M., El-Kaderi, H.M., Harris, C. T., & Gupta, R. B. (2015). Graphitic Biocarbon from Metal-Catalyzed Hydrothermal Carbonization of Lignin. *Industrial Engineering Chemistry Research,* 54(43) 10731-10739; doi.org/10.1021/acs.iecr.5b02614

Gao, P., Zhou, Y., Meng, F., Zhang, Y., Liu, Z., & Zhang, W. (2016). Preparation and characterization of hydrochar from waste eucalyptus bark by hydrothermal carbonization. *Energy,* 97, 238; doi.org/10.1016/j.energy.2015.12.123

Guo, Y., Yeh, T., Song, W., Xu, D., & Wang, S. (2015). A review of bio-oil production from hydrothermal liquefaction of algae. *Renewable and Sustainable Energy Rev*iew, 48, 776; doi.org/10.1016/j.rser.2015.04.049

Hadhoum, L., Balistrou, M., Burnens, G., Loubar, K., & Tazerout M (2016). Hydrothermal liquefaction of oil mill wastewater for bio-oil production in subcritical conditions. *Bioresource Technology*. 218 9; doi.org/10.1016/j.biortech.2016.06.054

Jain, A., Balasubramanian, R., & Srinivasan, M.P. (2016). Hydrothermal conversion of biomass waste to activated carbon with high porosity: A review. *Chemical Engineering Journal,* 283, 789–805; doi.org/10.1016/j.cej.2015.08.014

Jeong, H. M., Lee, J. W., Shin, W. H., Choi, Y. J., Shin, H. J, Kang, J. K., & Choi, J. W. (2011). Nitrogen-Doped Graphene for High-Performance Ultracapacitors and the Importance of Nitrogen-Doped Sites at Basal Planes. *Nano Letter*, 11, 2472–2477; doi.org/10.1021/nl2009058

Kambey, C. S. B, Campbell, I., Sondak, C. F. A, Nor, A.R.M, Lim, P.E., & Cook, E. J. C. (2020). An analysis of biosecurity frameworks' current status and future for the Indonesian seaweed industry. *Journal of Applied Phycology*, 32,2147–2160; doi.org/10.1007/s10811-019-02020-3.

Khan,T.A., Saud, A.S., Jamaric, S. S., Rahim, M. H., Park, J. W., & Kim, H. (2019). Hydrothermal carbonization of lignocellulosic biomass for carbon-rich material preparation: A review. Biomass and Bioenergy, 130, 105384; doi.org/10.1016/j.biombioe.2019.105384

Kim, S. S., Ly, H. V., Kim, J., Choi, J. H. & Woo, H. C. (2013). Thermogravimetric characteristics and pyrolysis kinetics of Alga Sagarssum sp. Biomass, *Bioresource Technology,* 139, 242; doi.org/10.1016/j.biortech.2013.03.192.

Kumar, A., Saini, K., Bhaskar, T., 2020. Hydochar and biochar: Production, physicochemical properties, and techno-economic analysis. *Bioresource Technol*ogy, 310, 123442; doi.org/10.1016/j.biortech.2020.123442.

Liu, Z., Zhang, F. S., & Wu, J. (2010). Characterization and application of chars produced from pinewood pyrolysis and hydrothermal treatment. *Fuel,* 89 (2) 510-514; doi.org/10.1016/j.fuel.2009.08.042

Luo, L., Chen, T., Li, Z., Zhang, Z., Zhao, W., & Fan (2018). Heteroatom self-doped activated biocarbon from fir bark and their excellent performance for carbon dioxide adsorption. *Journal of CO_2 Utilization,* 25, 89; doi.org/10.1016/j.jcou.2018.03.014

Li, D., Chen, l., Zhang, X., Ye, N., & Xing, F. (2011). Pyrolytic characteristics and kinetic studies of three kinds of red algae. *Biomass and Bioenergy,* 35, 1765; doi.org/10.1016/j.biombioe.2011.01.011.

Li, Y., Hagos, F.M., Chen, R., Qian, H., Mo, C., Di, J., Gai, X., Yang, R., Pan., G., & Shan., S. (2021). Rice husk hydrochars from metal chloride-assisted hydrothermal carbonization as biosorbents of organics from aqueous solution. *Bioresource and Bioprocessing,* 8**,** 99; doi.org/10.1186/s40643-021-00451-w.

Melo, C. A., Junior, F.H.S., Bisinoti, M. C., Moreira, A. B., & Ferreira, O. P. (2017). Transforming Sugarcane Bagasse and Vinasse Wastes into Hydrochar in the Presence of Phosphoric Acid: An Evaluation of Nutrient Contents and Structural Properties. *Waste and Biomass Valorization*, **8**, 1139–1151. doi.org/10.1007/s12649-016-9664-4

Mumme, J., Eckervogt, L., Pielert, J., Diakite, M., Rupp, F., & Kern, J. (2011). Hydrothermal carbonization of anaerobically digested maize silage. *Bioresource Technology,* 102 (19) 9255-926; doi.org/10.1016/j.biortech.2011.06.099

Patel, N., Acharya, B., & Basu, P. (2021). Hydrothermal Carbonization (HTC) of Seaweed (Macroalgae) for Producing Hydrochar. *Energies,* 14, 1805; doi.org/10.3390/en14071805.

Prakoso, T., Nurastuti, R., Hendriansyah, R., Rizkiana, J., Suantika, G., & Guan, G. (2018). Hydrothermal Carbonization of Seaweed for Advanced Biochar Production. *MATEC Web of Conferences* 156**,** 05012; doi.org/10.1051/matecconf/201815605012

Purnomo, A.H., Utomo, B.S.B, & Paul, N.(2020). Institutional arrangement for quality improvement of the Indonesian gracilaria seaweed. *AACL Bioflux*, 13(5), 2798–2806.

Reza, M. T., Andert, J., Wirth, B., Busch, D., Pielert, J., Lynam, J. G., & Mumme, J. (2014). Hydrothermal Carbonization of Biomass for Energy and Crop Production. *Applied Bioenergy,* 1, 11; dio.org/10.2478/apbi-2014-0001

Saleh, H. & Sebastian, E. (2020). Seaweed Nation: Indonesia's new growth sector. Australia-Indonesia Centre, 2, 1-8.

Satlewal, A., Agrawal, R., Bhagia, S , Sangoro, J. , & Ragauskas, S. J. (2018). Natural deep eutectic solvents for lignocellulosic biomass pretreatment: Recent developments, challenges, and novel opportunities. *Biotechnology Advances*, 36, 2032–2050; doi.org/10.1016/j.biotechadv.2018.08.009.

Schneider, D, Escala, M., Supawittayayothin, K., & Tippayawong, N. (2011). Characterization of biochar from hydrothermal carbonization of bamboo, *International Journal of Energy & Environmental Engineering,* 2(4), 647.

Shen, R., Lu, J., Yao, Z., Zhao, L., & Wu, Y. (2021). The hydrochar activation and bio-crude upgrading from hydrothermal treatment of lignocellulosic biomass, *Bioresource Technology,* 342, 125914; doi.org/10.1016/j.biortech.2021.125914

Smith, A. M. & Ross, A.B. (2016). Production of bio-coal, bio-methane, and fertilizer from seaweed via hydrothermal carbonization. *Algal Research*, 16, 1–11; doi.org/10.1016/j.algal.2016.02.026.

Speight, J. G. (2015). *Handbook of Petroleum Product Analysis*. Hoboken, NJ: Wiley. pp. 158–159.

Stemann, J., Erlach, B., & Ziegler, F., (2013). Hydrothermal carbonization of empty palm oil fruit bunches: laboratory trials, plant simulation, carbon avoidance, and economic

feasibility. *Waste and Biomass Valorization,* 4 (3), 441–454; doi.org/10.1007/s12649-012-9190-y

Tekin, K., Karagoz, S., & Bektas, S. (2014). A review of hydrothermal biomass processing. *Renewable and Sustainable Energy Review,* 40, 67; doi.org/10.1016/j.rser.2014.07.216

Titirici, M. M. (2013). *Sustainable Carbon Materials from Hydrothermal Processes* (New York: John Wiley & Sons) p.131.

Unrean, P., Lai Fui, B.C., Rianawati, E., & Acda, M., (2018). Comparative techno-economic assessment and environmental impacts of rice husk-to-fuel conversion technologies. *Energy*, 151, 581–593; doi.org/10.1016/j.energy.2018.03.112

Wang, T., Zhaia, Y., Zhuc, Y., Lia, C., & Guangming, G. (201). A review of the hydrothermal carbonization of biomass waste for hydrochar formation: Process conditions, fundamentals, and physicochemical properties, *Renewable and Sustainable Energy Reviews*, 90, 223–247; doi.org/10.1016/j.rser.2018.03.071

Wei, Y., Hong, J., & Ji, W. (2018). Thermal characterization and pyrolysis of digestate for phenol production. *Fuel*, 232, 141-146; doi.org/10.1016/j.fuel.2018.05.134

Xu, Q., Qian, Q., Quek, A., Ai, N., Zeng, G., & Wang, J. (2013). Hydrothermal Carbonization of Macroalgae and the Effects of Experimental Parameters on the Properties of Hydrochars. *ACS Sustainable Chemistry and Engineering,* , 1092-1101; doi.org/10.1021/sc400118f

Zhang, Z., Wang, K., Atkinson, J. D., Yan, X., Li, X., Rood, M. J., & Yan. (2012). Sustainable and hierarchical porous Enteromorpha prolifera based carbon for CO2 capture. *Journal of Hazardous Materials*, 229–230, 183–191; 10.1016/j.jhazmat.2012.05.094.

Zhang, Z., Zhu., Z., Shen, B., & Liu., L. (2019). Insights into biochar and hydrochar production and applications: A review. *Energy*, 171, 581-598; doi.org/10.1016/j.energy.2019.01.035

Zeng, G., Lou, S., Ying, H., Wu, X., Dou, X., Ai, N., & Wang, J. (2018). Preparation of Microporous Carbon from *Sargassum horneri* by Hydrothermal Carbonization and KOH Activation for CO_2 Capture. *Journal of Chemistry,* 2018, 4319149 11; doi.org/10.1155/2018/4319149